Scientific Herald of Uzhhorod University
Series "Physics"

Journal homepage: https://physics.uz.ua/en
Issue 53, 53-63
Received: 04/12/2023. Revised: 05/14/2023. Accepted: 06/01/2023

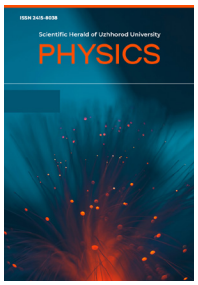

UDC 538.951
PACS 62.20.Dc, 62.20.Fe
DOI: 10.54919/physics/53.2023.53

Elastic-plastic properties of $Li_2B_4O_7$ determined by nanoindentation

Iryna Chobal

Assistant
Uzhhorod National University
88000, 3 Narodna Sq., Uzhhorod, Ukraine
https://orcid.org/0009-0002-5021-5184

Oleksandr Chobal*

PhD in Physical and Mathematical Sciences, Associate Professor
Uzhhorod National University
88000, 3 Narodna Sq., Uzhhorod, Ukraine
https://orcid.org/0000-0002-8042-8052

Yuliia Myslo

PhD in Physical and Mathematical Sciences, Associate Professor
Uzhhorod National University
88000, 3 Narodna Sq., Uzhhorod, Ukraine
https://orcid.org/0000-0001-6771-2844

Ivan Petryshynets

PhD in Technical Sciences, Senior Researcher
Institute of Materials Research of Slovak Academy of Sciences
04001, 47 Watsonova Str., Košice, Slovakia
https://orcid.org/0000-0001-8001-5349

Vasyl Rizak

Doctor of Physical and Mathematical Sciences, Professor
Uzhhorod National University
88000, 3 Narodna Sq., Uzhhorod, Ukraine
https://orcid.org/0000-0002-9177-0662

Suggested Citation:
Chobal I, Chobal O, Myslo Yu, Petryshynets I, Rizak V. Elastic-plastic properties of $Li_2B_4O_7$ determined by nanoindentation. *Sci Herald Uzhhorod Univ Ser Phys.* 2023;(53):53-63. doi: 10.54919/physics/53.2023.53

*Corresponding author

Abstract

Relevance. Crystalline and amorphous lithium tetraborate ($Li_2B_4O_7$) has a wide range of practical applications due to its physical properties. The knowledge of the mechanical characteristics of the surface layers of these materials, which are studied by nanoindentation, is necessary for optimising the technological processes for obtaining "optically perfect" samples.

Aim. A comparative study of the mechanical properties and deformation mechanisms of glassy and crystalline $Li_2B_4O_7$ samples in a wide range of applied loads.

Methodology. The elastic-plastic properties of crystalline and glassy lithium tetraborate were investigated using the multiple-loading cyclic nanoindentation method. The samples were measured at maximum loading forces of 50, 100, 150, 200, 250, 300, 350, 400, 450, and 500 mN. Four measurements (in the form of a 2x2 matrix) were made at a distance of 50 μm from each other on each sample and at each load. Young's modulus, hardness, and Poisson's ratio of $Li_2B_4O_7$ glass were also calculated using the Makishima-Mackenzie theory.

Results. The load-displacement curves and graphs of the dependence of the average contact pressure on the displacement of the diamond Berkovich indenter were obtained, which have a "smooth" shape and no anomalies associated with "pop-in" or "pop-out" effects. The indentation modulus (Young's modulus *E*) and hardness *H* of the studied samples were obtained from the experimental *P-h* load-displacement diagrams. The measured values mainly depend on the applied load or the contact depth of the indenter penetration into the crystalline and vitreous lithium tetraborate.

Conclusions. Both the hardness and Young's modulus of $Li_2B_4O_7$ glass are lower than those of the single crystal, indicating a lower resistance of amorphous lithium tetraborate to elastic and plastic deformations. The obtained experimental values of hardness and Young's modulus of $Li_2B_4O_7$ glass correlate well with the results of the calculation within the framework of the Makishima-Mackenzie theory. Multiple-loading cyclic nanoindentation leads to deformation densification of glassy $Li_2B_4O_7$ due to changes in the angles and lengths of chemical bonds, which leads to a decrease in the free volume in the medium-order structure of glass, as well as a change in the coordination of Boron atoms relative to Oxygen, i.e., the transformation of three-coordinated Boron into four-coordinated Boron

Keywords: lithium tetraborate crystals; Li_2O-$2B_2O_3$ glass; deformation densification; Young's modulus; hardness; phase transition

Introduction

The research interest in the superionic conductor lithium tetraborate ($Li_2B_4O_7$) is determined by its broad prospects for use in nonlinear optical and piezoelectric devices. Lithium tetraborate is a promising nonlinear material for laser frequency conversion, including for generating the fourth and fifth harmonics of Nd:YAG lasers [1] and sub-terahertz radiation [2]. In addition, following Sahil *et al.* [3] and Mehrabi *et al.* [4], $Li_2B_4O_7$ crystals (doped with various impurities) have wide application possibilities in radiation dosimetry. The study by J. Puebla *et al.* [5] indicates that other applications of $Li_2B_4O_7$ include surface and bulk acoustic wave devices, cellular phones, and data transmission devices. Lithium-borate glasses are of great interest due to their good ionic conductivity properties [6] and potential use in solid-state batteries [7; 8].

F. Pöhl [9] substantiated that indentation testing, in particular nanoindentation, is widely used to determine the local mechanical characteristics of materials and individual phases in multiphase materials. A. Gouldstone [10] found that it allows determining important mechanical parameters (e.g., hardness and Young's modulus) and energy characteristics of load-unload cycles, and greatly contributes to the understanding of mechanical behaviour on the nanometre scale, during which unique deformation phenomena often occur. Thus, previously, in [11; 12], nanoindentation of crystalline $Li_2B_4O_7$ was carried out in a limited range of applied loading forces. In particular, the authors of [11] recorded a discontinuity in the graph of the dependence (the so-called "pop-in" effect) of the indenter loading force on the depth of its penetration into the plane (100) of the lithium tetraborate crystal, which was explained by the nucleation of dislocations or possible phase transitions in the $Li_2B_4O_7$ crystal under compression. However, later, the authors of [12] did not observe the "pop-in" effect on the load-depth indentation curves in the same plane [100]. The corresponding experimental studies were conducted with only two loading forces, which

did not allow to fully study the dimensional effects of nanoindentation. Interestingly, the pop-in effect can also be caused by pressure-induced surface amorphisation of the crystal [13]. Given that reversible or irreversible amorphisation (depending on the magnitude of the external force) of lithium tetraborate crystals during bulk compression was previously reported [14], as well as the presence of conflicting literature data on mechanical properties and possible phase transformations under pressure, this study was conducted.

The study aims to conduct a comparative study of the mechanical properties and deformation mechanisms of glassy and crystalline $Li_2B_4O_7$ samples in a wide range of applied loads.

Materials and Methods

Experimental measurements were performed by cyclic nanoindentation with multiple loading with a maximum force of 50-500 mN and hold at the peak load for a certain time, which allows considering the viscoelastic component of the deformation and avoiding errors in determining elastic moduli from unloading curves [15; 16]. Lithium tetraborate was obtained according to the author's method [17] by gradual melting of pre-dewatered high-purity boron oxide B_2O_3 and lithium carbonate Li_2CO_3 in a platinum crucible in the air. Single crystals of $Li_2B_4O_7$ were grown by the Chokhralsky method in an air atmosphere in an HX-620 unit with automatic diameter control.

To obtain vitreous $Li_2B_4O_7$, the composition of which corresponded to the stoichiometric composition and contained a minimum number of impurities, a part of a single crystal of $Li_2B_4O_7$, which did not contain solid-phase and gas inclusions, was used as a starting material. It was melted in a platinum crucible in the air at a temperature of 1240-1290 K and then cooled in the quenching mode. To relieve thermal stresses, the glass removed from the crucible was annealed for 2-4 hours at 550-600 K. The glassy state of the obtained samples was confirmed by X-ray diffraction analysis, which confirmed the absence of characteristic peaks in the X-ray diffraction patterns that would indicate the presence of crystalline inclusions.

The samples used to study the mechanical properties were cut from crystalline and glassy $Li_2B_4O_7$ in the form of rectangular parallelepipeds with dimensions of about 5×5×10 mm. The orientation accuracy of the single-crystal samples relative to the crystallographic direction [100] was at least 0.5°. Both samples were ground and polished.

To determine the mechanical properties, indentation tests were performed on a Nanoindenter G200 using a Berkovich pyramidal diamond indenter. The nanoindentation procedure is performed by applying a load to the diamond indenter and recording the depth of its penetration into the material under test. This is done in the loading and unloading mode. Based on the obtained load-displacement curve, the elastic modulus and hardness of the sample material are automatically calculated following ISO 14577 [18] and the Oliver-Farr method [19].

The samples ($Li_2B_4O_7$ glass and single crystal of orientation [100]) were measured with a maximum force of 50, 100, 150, 200, 250, 300, 350, 400, 450, and 500 mN. Four measurements were made (in the form of a 2x2 matrix) at a distance of 50 μm from each other on each sample and under each load. The Poisson's ratios used for the calculation were 0.202 for vitreous [20] and 0.35 for crystalline $Li_2B_4O_7$ (averaged value [21]), the speed of approach to the surface was 10 nm/s, and the permissible drift rate was 0.05 nm/s.

The experiment was conducted by the method of multiple-loading cyclic nanoindentation with a trapezoidal function of the loading force (Fig. 1).

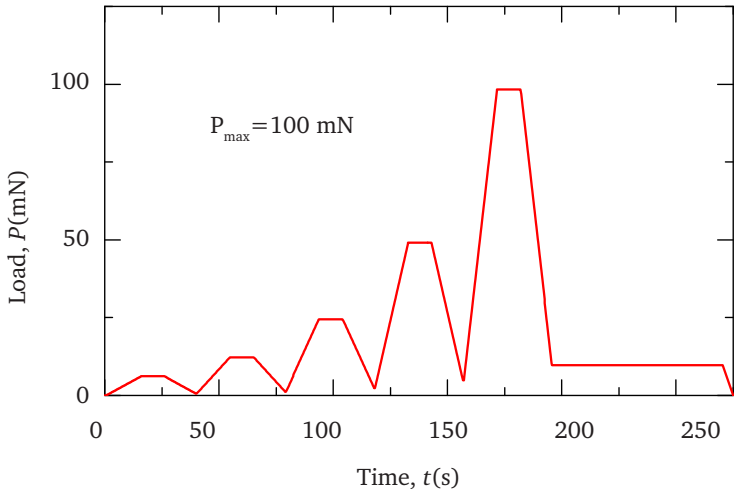

Figure 1. Typical load force dependence on indentation time used in this study
Source: compiled by the authors

Each test consisted of 5 loading and unloading cycles with a clear time interval: loading and unloading lasted 15 s, and peak force hold was 10 s (to avoid errors in determining experimental parameters due to the possible influence of viscoelastic and visco-plastic deformations). To calculate the hardness and elastic moduli of the studied materials during multiple nanoindentations in each indentation cycle, the NIGET software [22] was used within the framework of the Oliver-Farr technique [19].

For glassy lithium tetraborate, the elastic modulus E and Poisson's ratio ν were also calculated within the framework of Makishima and Mackenzie's theory [23; 24], which assumes that E is a function of the packing density of glass components V_i (determined by the ionic radii of the elements) and the dissociation energy G_i, which characterises the average strength of chemical bonds in glass:

$$E = 2V_t G_t, \quad (1)$$

$$\nu = 0.5 - \frac{1}{7.2V_t} \quad (2)$$

$$V_t = \frac{\rho}{M}\sum_i \quad X_i V_i, \quad (3)$$

$$G_t = \sum_i \quad X_i G_i, \quad (4)$$

where X_i – a molar fraction of the i-th glass component, ρ – density, M – a molar mass of the glass under study.

Results and Discussions

Figure 2 shows a typical dependence of the loading force (P) on the depth of penetration of the indenter (h) into the surface of the materials under study after 5 loading and unloading cycles with a maximum force of 100 mN in the crystallographic direction [100] of $Li_2B_4O_7$ crystals (Fig. 2a) and glassy $Li_2B_4O_7$ (Fig. 2b).

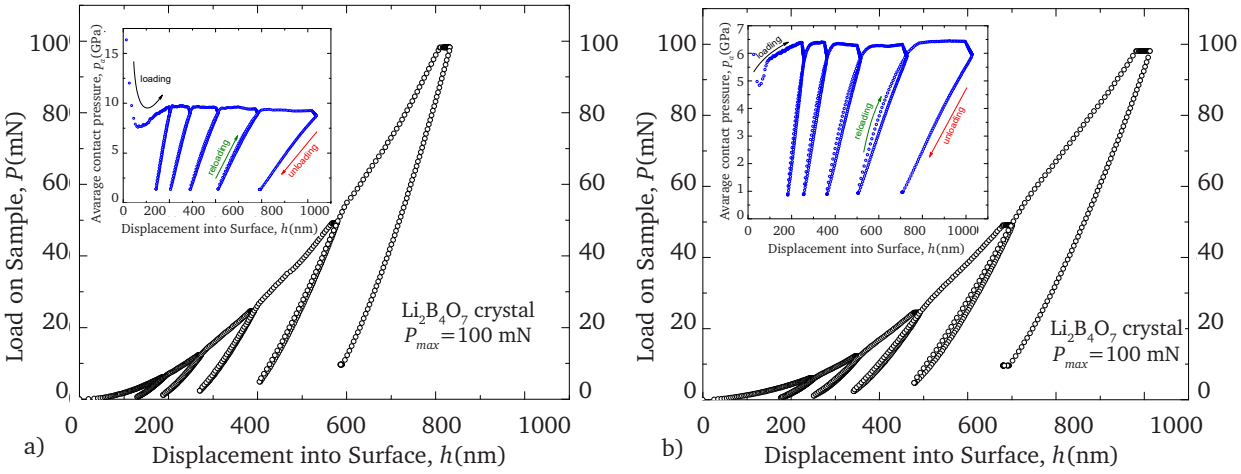

Figure 2. Dependence of the loading force (P) on the indenter displacement (h) into the surface (100) of a single crystal (a) and glassy $Li_2B_4O_7$ (b). The insets show the dependence of the average contact pressure on the indenter penetration depth

Source: compiled by the authors

The shape of the P-h diagrams is determined by the elastic, viscoelastic, and plastic properties of the materials under study. In particular, a preliminary conclusion can be made about the higher values of hardness and elastic moduli of crystalline $Li_2B_4O_7$, as well as a slight predominance of viscoelastic properties of vitreous lithium tetraborate (estimated by the area of hysteresis loops [25; 26]) based on the comparison of the obtained curves (Fig. 2). For a detailed analysis of the results obtained, the average contact pressure exerted on the sample during indentation was also estimated (insets in Fig. 2) using the ratio of the loading force P_i to the area of contact between the indenter and the material at the contact depth $A=f(h_c)$. It is worth noting that the indenter displacement h is automatically measured during the nanoindentation test, which is the sum of the contact depth h_c and the elastic deflection h_{el} of the sample surface at the contact edge. Therefore, to monitor the average contact pressure during the indenter movement, the method proposed by the authors of [27; 28] was used. In particular, the instantaneous value of the elastic deflection $h_{el(i)}$ of the sample surface near the contact perimeter was obtained by Eq:

$$h_{el(i)} = h_{el(max)}\left(\frac{P_i}{P_{max}}\right)^{\frac{1}{2}}, \quad (5)$$

where P_i, P_{max} – instantaneous and maximum loads on the sample, respectively; $h_{el(max)}$ – elastic deflection of the sample surface at the maximum load, determined according to the Oliver-Farr method [16]:

$$h_{el(max)} = \varepsilon\frac{P_{max}}{S}, \quad (6)$$

where ε – geometric constant (ε=0.75 for the Berkovich indenter used in this study), and S – contact stiffness of the specimen at the maximum load P_{max}.

The analysis of the obtained *P-h* diagrams and graphs of the dependence of the average contact pressure on the depth of penetration of the indenter into the surface of vitreous and crystalline $Li_2B_4O_7$ over the entire range of studied loads indicates their smooth shape and the absence of anomalies associated with "pop-in" or "pop-out" effects. At the initial stage of the curves, a directly proportional relationship between load and strain was recorded, indicating a purely elastic mechanism of deformation of lithium tetraborate in the nanoregion. The unloading curve at the initial stage, which describes the elastic recovery of the material, is also linear. According to the Oliver-Farr methodology [16], the slope of this *dP/dh* dependence determines the contact stiffness *S* at the point of maximum load (P_{max}, h_{max}):

$$S = \frac{dP}{dh}|_{h=h_{max}}. \quad (7)$$

By knowing the contact stiffness, it is possible to determine the reduced modulus E_r, which considers the deformation of both the indenter and the sample, and accordingly allows determining Young's indentation modulus *E* and the hardness *H* of the test sample [29]:

$$E_r = \frac{S\sqrt{\pi}}{2\beta\sqrt{A}}, \quad (8)$$

$$E = (1-\nu^2)\left[\frac{1}{E_r} - \frac{1-\nu_i^2}{E_i}\right]^{-1}, \quad (9)$$

$$H = \frac{P_{max}}{A}. \quad (10)$$

A – an area of contact between the indenter and the material; β – factor determined by the geometry of the indenter and equal to 1.034 for the Berkovich indenter; ν_i=0.07 and E_i=1140 GPa (Poisson's ratio and Young's modulus, respectively, for diamond indenter).

Figure 3 shows the results of *E* and *H* measurements obtained by analysing the *P-h* diagrams of nanoindentation during a series of tests with maximum loads of 50-500 mN. As can be seen from the figure, Young's modulus and hardness measurements of lithium tetraborate with a relatively small standard error of the experiment depend on the applied load (Figs. 3a, 3c) or the contact depth of the indenter (Figs. 3b, 3d). This is a manifestation of the so-called Indentational Size Effect (ISE), for which various mechanisms have been previously proposed [30; 31].

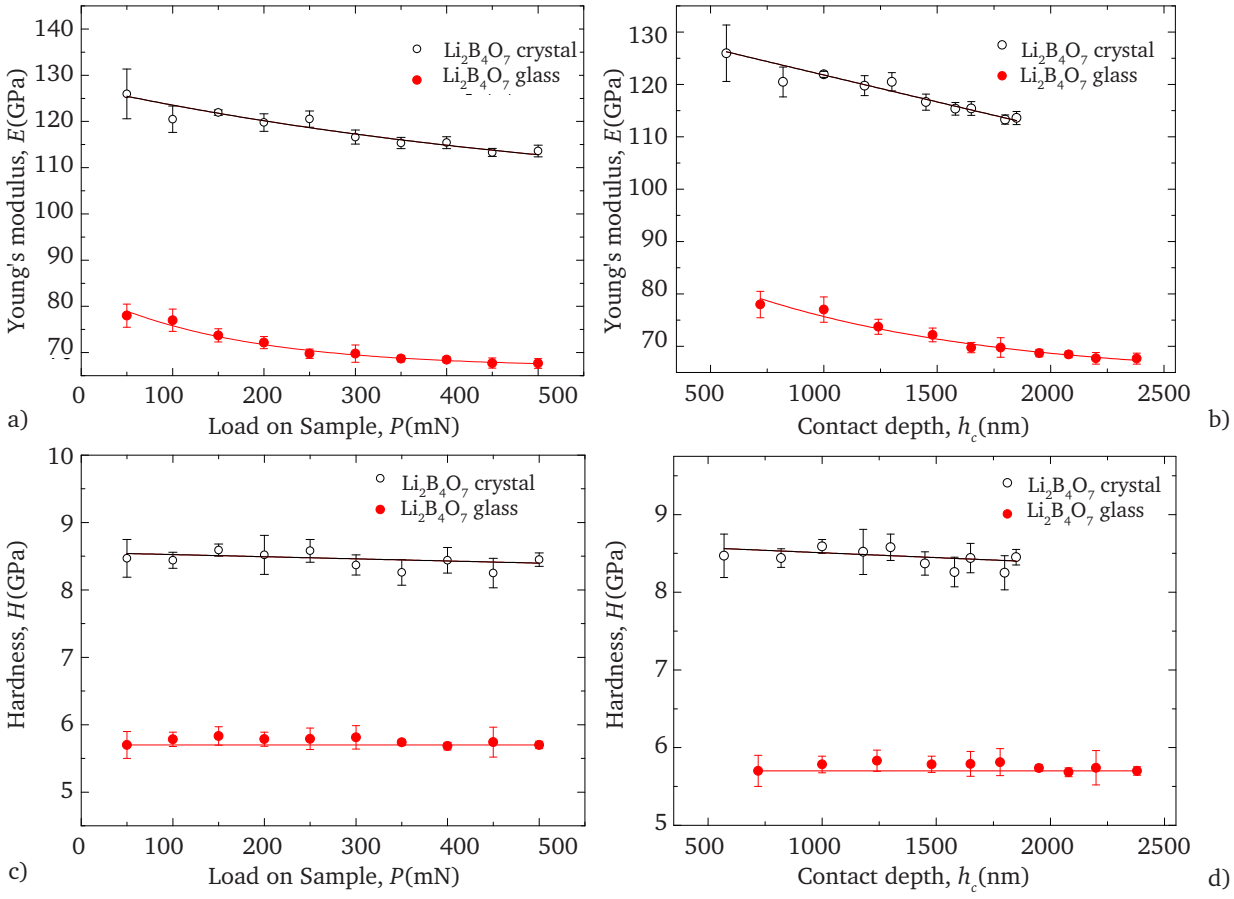

Figure 3. Young's modulus (a, b) and hardness (c, d) as a function of applied load (a, c) and contact depth (b, d) for the $Li_2B_4O_7$ glass and (100) plane of the single crystal

Source: compiled by the authors

As can be seen from Figures 3a, and 3b, the value of Young's modulus for both single crystal and glass samples is higher on the free surface and tends to decrease with increasing load and contact depth. For vitreous $Li_2B_4O_7$, a tendency to saturate the obtained E values with an increase in the penetration depth in the studied range was recorded. Study [32] reports the value of Young's modulus of the $Li_2B_4O_7$ crystal $E_{[100]}=12.8\cdot10^{10}$ Nm^{-2}, which was obtained from measuring ultrasonic wave velocities. The results of the E measurement by nanoindentation are in good agreement with these data, considering the size effects. Figures 3c, and 3d show the hardness versus loading force for single crystal and glassy lithium tetraborate samples. It was found that the hardness value for the $Li_2B_4O_7$ crystal in the studied load range decreases very slowly with increasing load, which also indicates a moderate ISE. At the same time, the hardness of lithium tetraborate glasses is practically independent of the indentation depth and applied load. In general, the obtained experimental values of H and E for crystalline lithium tetraborate are higher compared to the glassy one, which indicates a much lower resistance of $Li_2B_4O_7$ glass to elastic and plastic deformations.

Let us compare the experimentally obtained values of Young's modulus and hardness of glassy $Li_2B_4O_7$ with those calculated theoretically within the framework of Makishima and Mackenzie's theory [23; 24]. Lithium tetraborate glass consists of lithium oxide Li_2O and boron oxide B_2O_3 in a ratio of 1:2. According to S. Inaba [33], the values of the packing density coefficient V_{Li_2O} and dissociation energy G_{Li_2O} for lithium oxide are 8.0 cm^3/mol and 77.9 kJ/cm^3, respectively. The same parameters for boron oxide depend on the structural units from which the glass is formed. It is known from the study [34] that lithium tetraborate glass contains BO_3 and BO_4 structural units in equal proportions, i.e., the amount of tricoordinate boron relative to oxygen is equal to the amount of tetracoordinate boron ($N_3=N_4$). Accordingly, the dissociation energy and packing density coefficient of B_2O_3 has two values each: $G_3=15.6$ kJ/cm^3 [33], $V_3=15.2$ cm^3/mol [35] (three-coordinated boron atoms) and $G_{4\,t}=82.8$ kJ/cm^3 [33], $V_4=20.8$ cm^3/mol [35] (four-coordinated boron atoms). Therefore, to calculate the elastic modulus according to Y.B. Saddeek [36], the values of the dissociation energy and packing density were used, considering the ratio of fractions of three-coordinated and four-coordinated boron ($N_3=N_4=0.5$) in amorphous Li_2O-$2B_2O_3$:

$$G_{B_2O_3} = N_4G_4 + N_3G_3\,, \tag{11}$$

$$V_{B_2O_3} = N_4V_4 + N_3V_3\,. \tag{12}$$

Thus, using formulas (1-4) and (11-12), the value of Young's modulus for $Li_2B_4O_7$ glass was calculated – $E=67.2$ GPa, which is in full agreement with the experimentally obtained value of the indentation modulus within the measurement error. The calculated Poisson's ratio $\nu=0.25$ is slightly higher than the experimental value $\nu=0.202$ [20].

Considering the relationship between Young's modulus of an isotropic medium, Poisson's ratio and hardness:

$$H = \frac{(1-2\nu)}{6(1+\nu)}E, \tag{13}$$

the hardness of $Li_2B_4O_7$ glass $H=5.58$ GPa was also calculated, which almost completely coincides with the microhardness value obtained by nanoindentation.

The modulus of elasticity and hardness of amorphous and crystalline lithium tetraborate quantify the general variations in elastic and plastic deformation of materials under contact loading, but they do not fully describe the nature of the deformation process. A better understanding of the deformation features can be obtained by analysing the cyclic processes of multi-step loading and unloading within the energy approach [37; 38]. As a factor of mechanical losses during macroscopic fatigue tests, researchers usually use the ratio of the work W_{plast} spent on plastic deformation to the total work W_{total} consumed by the nanoindenter actuator: $\Psi=W_{plast}/W_{total}$. The proportion of plastic deformation energy (W_{plast}) in the work consumed by the nanoindenter actuator is determined by the area of the loop formed by the loading and unloading curves in one cycle [38]. As follows from the results obtained (Fig. 4), after five loading and unloading cycles, Ψ decreases for lithium tetraborate glass and remains almost constant for $Li_2B_4O_7$ single crystal over the number of cycles used in the experiment. In each loading-unloading cycle during multiple nanoindentations, the elastic modulus and hardness of lithium tetraborate glass were determined using the NIGET software [22] using the unloading curves (Fig. 2b). The results indicate that the hardness of glassy $Li_2B_4O_7$ increases with each indentation cycle from about 5.4 to 6.9 GPa, and Young's modulus varies between 81 and 92 GPa, showing an upward trend in some areas.

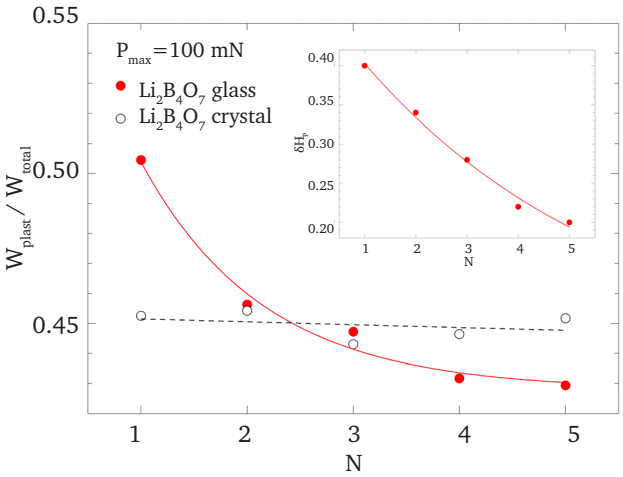

Figure 4. Variation W_{plast}/W_{total} during cyclic nanoindentation of $Li_2B_4O_7$ single crystal and glass. The inset shows the change in the plasticity parameter δH_p of glassy $Li_2B_4O_7$ during five nanoindentation cycles
Source: compiled by the authors

Thus, the observed decrease in the proportion of plastic strain energy in $Li_2B_4O_7$ glass can be qualified as the strengthening of the near-surface layers under the action of local loading. Knowing the *H/E* ratio in each nanoindentation cycle and the Poisson's ratio, the plasticity parameter δH_p of the material can be calculated by the equation [39]:

$$\delta H_P = 1 - 14.3(1 - \nu - 2\nu^2)H/E \ . \qquad (14)$$

Considering the increase in the *H/E* ratio with each subsequent indentation cycle, we conclude that the plasticity parameter of glassy $Li_2B_4O_7$ decreases (inset in Fig. 4), which is consistent with the previous conclusion based on the energy approach. Thus, the comparative analysis of the deformation mechanisms of crystalline and glassy lithium tetraborate indicates the dominance of the elastic deformation mechanism of crystalline $Li_2B_4O_7$, which does not depend on the number of indentation cycles. Instead, the contribution of the plastic component to the deformation of glassy $Li_2B_4O_7$ gradually decreases, transforming into an elastic and viscoelastic deformation mechanism.

The plastic deformation of glass is mainly determined by two competing mechanisms – glass densification under the indenter or plastic shear flows [40]. Given the relatively low value of the Poisson's ratio of $Li_2B_4O_7$ glass ($\nu \approx 0.2$), according to the results of [41], it can be concluded that the densification effect will be dominant compared to the processes of plastic shear flow in the glass under study. Also, the *H/E* ratio for the glass under study is about 0.1. This indicates the covalent nature of the chemical bonds and a very low probability of plastic shear according to [42]. At the same time, the obtained estimates of the average pressure generated in the contact plane (Fig. 2b) of vitreous $Li_2B_4O_7$ with the indenter indicate the occurrence of variable contact pressure in the range of 1-6.5 GPa during loading and unloading. This pressure corresponds to areas I, and II of hydrostatic compression of lithium tetraborate glass in [43], where it was concluded that in these intervals glass compaction processes occur due to topological variations in the angles and lengths of chemical bonds, which leads to a decrease in the free volume, as well as the transformation of three-coordinated boron into four-coordinated boron.

Finally, the possibility of amorphisation of crystalline $Li_2B_4O_7$ in the process of nanoindentation is evaluated. The average contact pressure during the indentation of a single crystal of lithium tetraborate (inset in Fig. 2a) is about 15 GPa at the beginning of indentation, and then gradually decreases, reaching constant values of about 10 GPa, and decreases to 1-2 GPa during unloading. Thus, comparing these values with the results of [14], we conclude that the indenter pressure is insufficient for the amorphization of the crystalline sample, requiring more than 17 GPa for the reverse amorphization of crystalline $Li_2B_4O_7$. This conclusion is qualitatively consistent with the results of [12], where no features associated with phase transformations were found on the nanoindentation curves of lithium tetraborate crystals in the (100) plane.

Conclusions

The elastic and plastic properties of crystalline and vitreous lithium tetraborate have been investigated by cyclic nanoindentation with repeated loading with a maximum force of 50-500 mN. The load-unload curves depending on the displacement of the diamond indenter and the graphs of the average contact pressure dependence were obtained, which have a smooth shape and no anomalies associated with "pop-in" or "pop-out" effects. The values of the indentation modulus (Young's modulus *E*) and the hardness *H* of the studied samples were obtained from the experimental

P-h diagrams. It is shown that the measured values mainly depend on the applied load or the contact depth of the indenter penetration into crystalline and glassy $Li_2B_4O_7$. The experimentally obtained parameters of mechanical deformation of lithium tetraborate glass are in good agreement with the theoretically calculated hardness, elastic modulus, and Poisson's ratio within the framework of Makishima and Mackenzie's theory. In general, the obtained experimental values of *H* and *E* for lithium tetraborate crystals are higher compared to the same parameters for glasses of the same composition, which indicates a much lower resistance of glassy $Li_2B_4O_7$ to elastic and plastic deformations.

The contrasting evolution of the relative work of plastic deformation and the plasticity parameter of the studied samples during cyclic nanoindentation indicates significantly different mechanisms of their deformation. In particular, repeated loading leads to densification of glassy $Li_2B_4O_7$ along with an increase in its hardness. These processes occur mainly due to the variation of the angles and lengths of chemical bonds, which leads to a decrease in the free volume in the medium-order structure of glass, as well as a change in the coordination of boron atoms relative to oxygen, i.e., the transformation of three-coordinated boron into four-coordinated boron. A comparative analysis of the deformation processes of glassy and crystalline lithium tetraborate, as well as estimates of the average contact pressure, indicate that the amorphization of crystalline lithium tetraborate does not occur during nanoindentation. At the same time, direct structural studies of lithium tetraborate under high pressure using synchrotron X-rays seem promising.

Conflict of Interest

The authors declare no conflict of interest.

Acknowledgements

The authors are sincerely grateful to Prof. Vadym Holovey, PhD, for kindly providing samples for the study.

References

[1] Komatsu R, Sugawara T, Sassa K, Sarukura N, Liu Z, Izumida S, *et al*. Growth and ultraviolet application of $Li_2B_4O_7$ crystals: Generation of the fourth and fifth harmonics of Nd:Y3Al5O12 lasers. *Appl Phys Lett*. 1997;70(26):3492-4. doi: 10.1063/1.119210.

[2] Ezhov D, Turgeneva S, Nikolaev N, Mamrashev A, Mikerin S, Minakov F, *et al*. The potential of sub-THz-wave generation in $Li_2B_4O_7$ nonlinear crystal at room and cryogenic temperatures. *Crystals*. 2021;11(11):1321. doi: 10.3390/CRYST11111321.

[3] Sahil, Kumar R, Yadav MK, Kumar P. OSL and TA-OSL properties of $Li_2B_4O_7$:Al for radiation dosimetry. *J Alloys Compd*. 2022;908:164628. doi: 10.1016/J.JALLCOM.2022.164628.

[4] Mehrabi M, Zahedifar M, Hasanloo S, Nikmanesh H, Gheisari R, Li Y. Preparation and characterization of $Li_2B_4O_7$ nanoparticles co-doped with Mg and Cu for thermoluminescence dosimetry of gamma-rays. *Radiat Phys Chem*. 2022;194:110057. doi: 10.1016/J.RADPHYSCHEM.2022.110057.

[5] Puebla J, Hwang Y, Maekawa S, Otani Y. Perspectives on spintronics with surface acoustic waves. *Appl Phys Lett*. 2022;120(22):220502. doi: 10.1063/5.0093654.

[6] Wohlmuth D, Epp V, Bernhard Stanje, Welsch AM, Behrens H, Wilkening M. High-energy mechanical treatment boosts ion transport in nanocrystalline $Li_2B_4O_7$. *J Am Ceram Soc*. 2016;99(5):1687-93. doi: 10.1111/JACE.14165.

[7] Han X, Zhou W, Chen M, Luo L, Gu L, Zhang Q, *et al*. Liquid-phase sintering enabling mixed ionic-electronic interphases and free-standing composite cathode architecture toward high energy solid-state battery. *Nano Res*. 2022;15(7):6156-67. doi: 10.1007/s12274-022-4242-5.

[8] Deng R, Tao J, Zhong W, Wen L, Yang Y, Li J, *et al*. Tri-functionalized $Li_2B_4O_7$ coated $LiNi_{0.5}Co_{0.2}Mn_{0.3}O_2$ for boosted performance lithium-ion batteries. *J Alloys Compd.* 2023;940:168767. doi: 10.1016/j.jallcom.2023.168767.

[9] Pöhl F. Pop-in behaviour and elastic-to-plastic transition of polycrystalline pure iron during sharp nanoindentation. *Sci. Rep*. 2019;9:15350. doi: 10.1038/s41598-019-51644-5.

[10] Gouldstone A, Chollacoop N, Dao M, Li J, Minor AM, Shen YL. Indentation across size scales and disciplines: Recent developments in experimentation and modelling. *Acta Mater*. 2007;55(12):4015-39. doi: 10.1016/j.actamat.2006.08.044.

[11] Stus NV, Dub S, Stratiychuk DA, Lisnyak VV. Pop-in effect at nanoindentation of lithium tetraborate (100) face. *J Alloys Compd*. 2005;403(1-2):305-7. doi: 10.1016/j.jallcom.2005.04.205.

[12] Gurga A, Juliano T, Gogotsi Y, Dub S, Stus N, Stratiichuk D, *et al*. The mechanical properties of lithium tetraborate (100), (011) and (112) faces. *Mater Lett*. 2007;61(3):770-3. doi: 10.1016/j.matlet.2006.05.058.

[13] Nazarov MV, Nazarova TA, Dub SN, Banini GK. SEM and AFM studies on micro- and nanoindentation of material. *Microscopy Analysis*. 2003;9:13-5.

[14] Li Y, Lan G. Pressure-induced amorphization study of lithium diborate. *J Phys Chem Solids*. 1996;57(12):1887-90. doi: 10.1016/S0022-3697(96)00081-9.
[15] Chudoba T, Richter F. Investigation of creep behaviour under load during indentation experiments and its influence on hardness and modulus results. *Surf Coat Technol*. 2001;148(2-3):191-8. doi: 10.1016/S0257-8972(01)01340-8.
[16] Briscoe BJ, Fiori L, Pelillo E. Nano-indentation of polymeric surfaces. *J Phys D: Appl Phys*. 1998;31(19):2395-405. doi: 10.1088/0022-3727/31/19/006.
[17] Holovey VM, Puga PP, Turok II, Holovey MI, inventors; Institute of Electron Physics of the National Academy of Sciences of Ukraine, patent holder. Method for growth of single crystals of lithium tetraborate [Internet]. Patent of Ukraine No. 34204. 2001 Feb 15 [cited 16 Jan 2023]. Available from: https://sis.nipo.gov.ua/uk/search/detail/342653/.
[18] ISO 14577-1:2002 – Metallic materials – Instrumented indentation test for hardness and materials parameters – Part 1: Test method. [Internet]. 2002 [cited 2023 May 15]. Available from: https://www.iso.org/standard/30104.html.
[19] Oliver W, Pharr G. An improved technique for determining hardness and elastic modulus using load and displacement sensing indentation experiments. *J Mater Res*. 1992;7:1564-83. doi: 10.1557/JMR.1992.1564.
[20] Gaafar M, El-Batal F, El-Gazery M, Mansour S. Effect of doping by different transition metals on the acoustical properties of alkali borate glasses. *Acta Phys Pol, A*. 2009;115(3):671-8. doi: 10.12693/APhysPolA.115.671.
[21] Goldstein RV, Gorodtsov VA, Lisovenko DS, Volkov MA. Auxetics among 6-constant tetragonal crystals. *Lett Mater*. 2015;5(4):409-13. doi: 10.22226/2410-3535-2015-4-409-413.
[22] Campbell AC, Grolich P, Šlesinger R. Niget: Nanoindentation general evaluation tool. *SoftwareX*. 2019;9:248-54. doi: 10.1016/j.softx.2019.03.001.
[23] Makishima A, Mackenzie J. Direct calculation of Young's modulus of glass. *J Non-Cryst Solids*. 1973;12(1):35-45. doi: 10.1016/0022-3093(73)90053-7.
[24] Makishima A, Mackenzie J. Calculation of bulk modulus, shear modulus and Poisson's ratio of glass. *J Non-Cryst Solids*. 1975;17(2):147-57. doi: 10.1016/0022-3093(75)90047-2.
[25] Nowicki M, Richter A, Wolf B, Kaczmarek H. Nanoscale mechanical properties of polymers irradiated by UV. *Polymer*. 2003;44(21):6599-606. doi: 10.1016/S0032-3861(03)00729-8.
[26] Gilbert JL, Cumber J, Butterfield A. Surface micromechanics of ultrahigh molecular weight polyethylene: Microindentation testing, crosslinking, and material behavior. *J Biomed Mater Res*. 2002;61(2):270-81. doi: 10.1002/jbm.10143.
[27] Novikov NV, Dub SN, Milman YV, Gridneva IV, Chugunova SI. Application of nanoindentation method to study a semiconductor-metal phase transformation in silicon. *J Superhard Mater*. 1996;18:32-40.
[28] Dub S, Novikov N, Milman Y. The transition from elastic to plastic behaviour in an Al-Cu-Fe quasicrystal studied by cyclic nanoindentation. *Philos Mag A*. 2002;82(10):2161-72. doi: 10.1080/01418610208235725.
[29] Agilent Technologies. Nano indenter G200 User manual. [Internet]. 2012 [cited 2022 Dec 11]. Available from: https://www.manualslib.com/manual/1254115/Agilent-Technologies-Nano-Indenter-G200.html.
[30] Weaver MA, Stevenson M, Bradt RC. Knoop microhardness anisotropy and the indentation size effect on the (100) of single crystal NiAl. *Mater Sci Eng*. 2003;345(1-2):113-7. doi: 10.1016/S0921-5093(02)00454-9.
[31] Mukhopadhyay NK, Paufler P. Micro- and nanoindentation techniques for mechanical characterisation of materials. *Int Mater Rev*. 2006;51(4):209-45. doi: 10.1179/174328006X102475.
[32] Sidek H, Saunders G, James B. The pressure and temperature dependences of the elastic behaviour of lithium tetraborate. *J Phys Chem Solids*. 1990;51(5):457-65. doi: 10.1016/0022-3697(90)90184-H.
[33] Inaba S, Fujino S, Morinaga K. Young's modulus and compositional parameters of oxide glasses. *J Am Ceram Soc*. 2004;82(12):3501-7. doi: 10.1111/j.1151-2916.1999.tb02272.x.
[34] Adamiv VT. Thermal properties of alkaline and alkaline-earth borate glasses. *Funct Mater*. 2013;20(1):52-8. doi: 10.15407/fm20.01.052.
[35] Inaba S, Oda S, Morinaga K. Heat capacity of oxide glasses at high temperature region. *J Non-Cryst Solids*. 2003;325(1-3):258-66. doi: 10.1016/S0022-3093(03)00315-6.
[36] Saddeek YB. Structural analysis of alkali borate glasses. *Phys B*. 2004;344(1-4):163-75. doi: 10.1016/j.physb.2003.09.254.
[37] Cheng Y, Cheng C. Scaling, dimensional analysis, and indentation measurements. *Mater Sci Eng: R: Reports*. 2004;44(4-5):91-149. doi: 10.1016/j.mser.2004.05.001.

[38] Attaf M. New ceramics related investigation of the indentation energy concept. *Mater Lett*. 2003;57(30):4684-93. doi: 10.1016/S0167-577x(03)00375-6.
[39] Milman Y, Galanov B, Chugunova S. Plasticity characteristic obtained through hardness measurement. *Acta Metall Mater*. 1993;41(9):2523-32. doi: 10.1016/0956-7151(93)90122-9.
[40] Kilymis DA, Delaye J. Deformation mechanisms during nanoindentation of sodium borosilicate glasses of nuclear interest. *J Chem Phys*. 2014;141(1):014504. doi: 10.1063/1.4885850.
[41] Rouxel T, Ji H, Guin JP, Augereau F, Rufflé B. Indentation deformation mechanism in glass: Densification versus shear flow. *J Appl Phys*. 2010;107(9):094903. doi: 10.1063/1.3407559.
[42] Wang JG, Choi BW, Nieh TG, Liu CT. Crystallization and nanoindentation behavior of a bulk Zr-Al-Ti-Cu-Ni amorphous alloy. *J Mater Res*. 2000;15(3):798-807. doi: 10.1557/JMR.2000.0114.
[43] Lee SK, Eng PJ, Mao H, Meng Y, Shu J. Structure of alkali borate glasses at high pressure: B and LiK-Edge inelastic X-Ray scattering study. *Phys Rev Lett*. 2007;98(10):105502. doi: 10.1103/PhysRevLett.98.105502.

Пружно-пластичні властивості $Li_2B_4O_7$ досліджені шляхом наноіндентування

Ірина Василівна Чобаль
Асистент
Ужгородський національний університет
88000, пл. Народна, 3, м. Ужгород, Україна
https://orcid.org/0009-0002-5021-5184

Олександр Ілліч Чобаль
Кандидат фізико-математичних наук, доцент
Ужгородський національний університет
88000, пл. Народна, 3, м. Ужгород, Україна
https://orcid.org/0000-0002-8042-8052

Юлія Михайлівна Мисло
Кандидат фізико-математичних наук, доцент
Ужгородський національний університет
88000, пл. Народна, 3, м. Ужгород, Україна
https://orcid.org/0000-0001-6771-2844

Іван Петришинець
Кандидат технічних наук, провідний науковий співробітник
Інститут матеріалознавства Словацької Академії Наук
04001, вул. Ватсонова, 47, м. Кошице, Словаччина
https://orcid.org/0000-0001-8001-5349

Василь Михайлович Різак
Доктор фізико-математичних наук, професор
Ужгородський національний університет
88000, пл. Народна, 3, м. Ужгород, Україна
https://orcid.org/0000-0002-9177-0662

Анотація

Актуальність. Кристалічний і аморфний тетраборат літію ($Li_2B_4O_7$) має широкі можливості практичного застосування завдяки своїм фізичним властивостям. Знання механічних характеристик поверхневих шарів цих матеріалів, що досліджуються шляхом наноіндентування, є важливим для оптимізації технологічних процесів отримання «оптично ідеальних» зразків.

Мета. Порівняльне вивчення механічних властивостей і механізмів деформації склоподібних та кристалічних зразків $Li_2B_4O_7$ в широкому діапазоні прикладених навантажень.

Методологія. Пружно-пластичні властивості кристалічного та склоподібного тетраборату літію досліджено методом багаторазового циклічного наноіндентування. Зразки вимірювали за допомогою максимальної сили навантаження 50, 100, 150, 200, 250, 300, 350, 400, 450 та 500 мН. Виконано чотири вимірювання (у вигляді матриці 2x2) на відстані 50 мкм одне від одного на кожному зразку та при кожному навантаженні. Модуль Юнга, твердість і коефіцієнт Пуассона скла $Li_2B_4O_7$ також було розраховано в рамках теорії Makishima-Mackenzie.

Результати. Отримано криві навантаження-розвантаження та графіки залежності середнього контактного тиску від переміщення алмазного індентора Берковича, що мають «гладку» форму та відсутність аномалій, які пов'язують з «pop-in» або «pop-out» ефектами. Із експериментальних *P-h* діаграм навантаження – переміщення отримано значення модуля індентування (модуль Юнга *E*) і значення твердості *H* досліджуваних зразків. Виміряні значення переважно залежать від прикладеного навантаження або контактної глибини проникнення індентора в кристалічний і склоподібний тетраборат літію.

Висновки. Як твердість, так і модуль Юнга скла $Li_2B_4O_7$ є меншими порівняно з відповідними даними монокристалу, що вказує на нижчу стійкість аморфного тетраборату літію до пружних і пластичних деформацій. Отримані експериментальні значення твердості та модуля Юнга скла $Li_2B_4O_7$ добре корелюють з результатами розрахунку в рамках теорії Makishima-Mackenzie. Багаторазове циклічне наноіндентування призводить до деформаційного ущільнення склоподібного $Li_2B_4O_7$ за рахунок зміни кутів і довжин хімічних зв'язків, що веде до зменшення вільного об'єму в структурі середнього порядку скла, а також зміни координації атомів Бору відносно Оксигену, тобто перетворення три-координованого Бору в чотири-координований

Ключові слова: кристали тетраборату літію; скло Li_2O-$2B_2O_3$; деформаційне ущільнення; модуль Юнга; твердість; фазовий перехід